WAVE FORCES ON A WAVEMAKER. SPH SIMULATION AND COMPARISON WITH ANALYTIC RESULTS

Jose M. Grassa[(1)]
[(1)]Centro de Estudios de Puertos y Costas, CEDEX, Antonio Lopez 81, 28026 Madrid, Spain,
phone: +34 91 3357610; fax: +34 91 3357622; e-mail: Jose.M.Grassa@cedex.es

ABSTRACT

Knowledge of wave forces on a wavemaker during experiments is an important question for the design of structural and driving system design of such elements. Also, it may be useful for active wave absorption of reflected waves and it may be considered as a very simple case of study of wave forces on a structure. Within a systematic study of a numerical SPH wave flume, this paper uses a simple procedure for obtaining such forces representing the boundary of the flume and, hence, the wave maker, by means of repulsive force boundary particles as proposed by Monaghan (1994). While other formulations for force boundaries do exist that provide a smooth boundary force field, Monaghan (1999) and other approaches like mirror particles may enable a better approximation of essential mathematical boundary conditions, this simplest implementation has some interest because it mimics in a physical way molecular forces, is easy to implement and may be applied in a generalized system without the need to consider special cases. Some aspects of the noise that appears in the simulations is discussed, and numerical results are compared with analytic results concluding that SPH may provide a rather appropriate evaluation of the force for the studied conditions, if the distance between boundary particles is made shorter than the initial distance between fluid particles while keeping a radius of influence of the boundary force of the order of magnitude of fluid particles separation, in order to reduce the added mass effect associated with this boundary condition. Numerical experiments have been conducted at three resolutions obtaining satisfactorily converging results that may imply that not an extreme resolution is needed at least in this case, an important fact given the computational cost of the method. Even if the boundary method requires an increased number of boundary particles, the dimensionality of the boundary is lower than that of the experiment and therefore this may not be a severe computational constraint in most cases.

Keywords: maritime hydraulics, wavemaker, wave forces, numerical model, SPH

1 INTRODUCTION

While the development of Computational Hydraulics has allowed the intensive use of numerical techniques in maritime engineering for the study of problems like wave propagation and disturbance in harbours, the study of stability and functional aspects of maritime structures continues to rely mainly on physical modelling and derived empirical methods. Even if some analytical solutions do exist for simple geometrical and physical cases, phenomena like wave overtopping is usually out of reach of such methods. There is no doubt of the interest as a basis for innovation in maritime engineering of numerical methods that may complement and even extend the physical experiments. A promissory way is the progressive application of more general CFD techniques on varied geophysical domains allowing the study of new typologies of structures as well as of construction procedures at the sea, of a fundamental importance from both cost and safety points of view, where limited numerical research has been conducted due to the complexity of the related dynamic processes.

The method SPH – see Monaghan (2005) for an up to date complete review is a mesh free Lagrangian technique, simple and flexible, that may be applied – but is not restricted - to the numerical solution of the Euler or Navier – Stokes equations for free surface flows, Monaghan (1994). Since 2001 the method has been applied by maritime hydraulics specialists to several problems including even 3D wave-like forces on structures, see Gomez – Gesteira and Dalrymple (2003), (2004). In the frame of the validation of an SPH wave flume, this paper is centred on the evaluation of simulated wave forces on a wave maker, a simple example of wave forces on a structure that has not been found in the existing literature. Such force is readily available from the simulation results and its comparison with experimental or analytic results may allow a judgment of the quality of the approximation and to analyze some of its properties. Furthermore, the availability of real time information on wave forces on a wave maker may be of use in some approaches to active absorption of reflected waves during experiments.

The paper organization is as follows: first, a very short introduction to the principles of the SPH method is made, including some details regarding the boundary condition used. A pseudo – hydrostatic simulation on a rectangular container is then presented, allowing to assess the accuracy and behaviour of the boundary force to be used to evaluate forces on the wave maker. The numerical wave generation experiment is next described, including setup, results analysis and comparison with analytical results. The same experiment is performed with three different resolutions in order to assess the convergence of results. Finally, relevant conclusions are presented as well as ideas for future work.

2 SPH METHOD, BOUNDARY CONDITIONS AND FORCE EVALUATION

SPH may be considered as a generic interpolation technique for field functions and its derivatives on continuous media, alternative to e.g., finite differences, and then applicable to the discretization of conservation equations on a basis of discrete elements - particles - that represent the media and move with it transporting its properties in a lagrangian manner. From its (exact) integral representation, an arbitrary field function $\boldsymbol{A(r)}$ is approximated in discrete form in a material media represented by particles of volume $\boldsymbol{V_b}$, mass $\boldsymbol{m_b}$ and density $\boldsymbol{\rho_b}$ as:

$$A(r_a) = \sum_b \frac{m_b}{\rho_b} A(r_b)\, W(r_a - r_b, h) \tag{1}$$

Where $\boldsymbol{r}$ is the position vector, $\boldsymbol{b}$ is a set of particles in the neighbourhood of $\boldsymbol{a}$ and $\boldsymbol{W}$ is a smoothing function kernel that approximates the Dirac Delta function when the smoothing

length, $\boldsymbol{h}$ – a measure of the resolution of the model-, tends to zero. A model - form for $\boldsymbol{W}$ is a normalized Gaussian shape function or polynomial spline function not null only within a radius $\boldsymbol{n\ h}$ with n being a small integer (2 – 3 in practice). From (1) it is easy to develop, with some additional restraints, an expression for the function derivative using the function value and the analytical (usually) derivative of the kernel:

$$A'(r_a) = -\sum_b \frac{m_b}{\rho_b} A(r_b)\, W'(r_a - r_b, h) \tag{2}$$

Using (1) and (2) and enforcing symmetry for ensuring conservation, mass continuity and acceleration equations may be written in the following common form:

$$\begin{aligned} \frac{dv_a}{dt} &= -\sum_b m_b \left(\frac{p_b}{\rho_b^2} + \frac{p_a}{\rho_a^2} + \Pi_{ab} \right) \nabla W_{ab} \\ \frac{d\rho_a}{dt} &= \sum_b m_b \left(v_a - v_b \right) \cdot \nabla W_{ab} \end{aligned} \tag{3}$$

Being $\boldsymbol{v}$ the velocity, $\boldsymbol{p}$ the pressure and $\boldsymbol{\nabla}$ the spatial gradient of the kernel function. $\boldsymbol{\Pi}$ term represents usually and artificial viscosity term that allows for the treatment of shocks:

$$\begin{aligned} \Pi_{ab} &= \begin{cases} \dfrac{-\alpha\, \bar{c}_{ab} \mu_{ab} + \beta \mu_{ab}^2}{\bar{\rho}_{ab}}, & v_{ab} \cdot r_{ab} < 0 \\ 0, & v_{ab} \cdot r_{ab} > 0 \end{cases} \\ \mu_{ab} &= \frac{h v_{ab} \cdot r_{ab}}{r_{ab}^2 + (0.1h)^2} \end{aligned} \tag{4}$$

Where $\boldsymbol{\alpha}$, $\boldsymbol{\beta}$ are parameters (usually $\boldsymbol{\alpha}$ = 0.01 and $\boldsymbol{\beta}$ = 0) and $\boldsymbol{c_{ab}}$ is an averaged value of the speed of sound on the fluid.

The expressions (3), plus a kinematics equation for updating particle positions, form a system of ordinary differential equations that may be integrated on time advancing the simulation of the flow, including a closure condition that relates pressure and evolving density in the slightly compressible formulation of Monaghan (1994):

$$P = \frac{c_s^2 \rho_0}{\gamma} \left(\left(\frac{\rho}{\rho_0} \right)^{\gamma} - 1 \right) \tag{5}$$

Where $\boldsymbol{c_s}$ is the speed of sound and $\boldsymbol{\gamma}$ = 7. Provided $\boldsymbol{c_s}$ is taken around ten times the maximum flow speed, maximum variation of density remains in the order of 1%. An XSPH correction in the kinematics equation proposed by Monaghan (1992) is usually also used in the context of free surface flows.

There exist several alternative for establishing boundary conditions on an SPH simulation. A first one is using mirror or ghost particles with properties adjusted according to the real fluid particles for simulating essential conditions: continuity, reflection, no slip, …. Monaghan (1994) proposed a very simple force boundary condition that simulates the boundary using particles that exert a repulsive force per unit mass on fluid particles in its environment according to:

$$f(r) = D \left(\left(\frac{r_0}{r} \right)^{p_1} - \left(\frac{r_0}{r} \right)^{p_2} \right) \frac{\vec{r}}{r^2} \tag{6}$$

Being $\boldsymbol{r_0}$ the radius of application of the force, $\boldsymbol{p_1} > \boldsymbol{p_2}$ coefficients (usual values are $\boldsymbol{p_1}$ = 4, $\boldsymbol{p_2}$ = 2) and D a dimensional coefficient. Such force, modelled after molecular dynamics forces, represents an elastic model and, as a drawback, has the property of producing a 'roughness' of the boundary in such a way that a fluid particle moving parallel to a boundary formed by a series of such particles does not experiment a constant force. Even if an improved

boundary model force by Monaghan (2003) avoids this problem – at the cost of an slightly more complicated implementation – here a practical improvement for this basic boundary has been used, by reducing the spacing between boundary particles while keeping the radius of application of the force. Figure 1 shows the effect, on the shape of the force field, of such strategy, for a radius of influence unity and particle spacing of 1, ½ and ¼. It may be seen that the isolines of the force field potential (here represented in the interval 0 – 20 with $\boldsymbol{D}$ = 1) become nearly boundary parallel for spacing 1/2 and higher, producing therefore a force nearly constant on a particle moving parallel to the boundary. In the opposite, case – similar radius of action and spacing - it is clear that fluid particles may accommodate in the force field 'wells' requiring a not null boundary parallel force for moving from this equilibrium position and thus producing an added mass effect. The configuration with ¼ spacing will be used on the force test in order to avoid such effect.

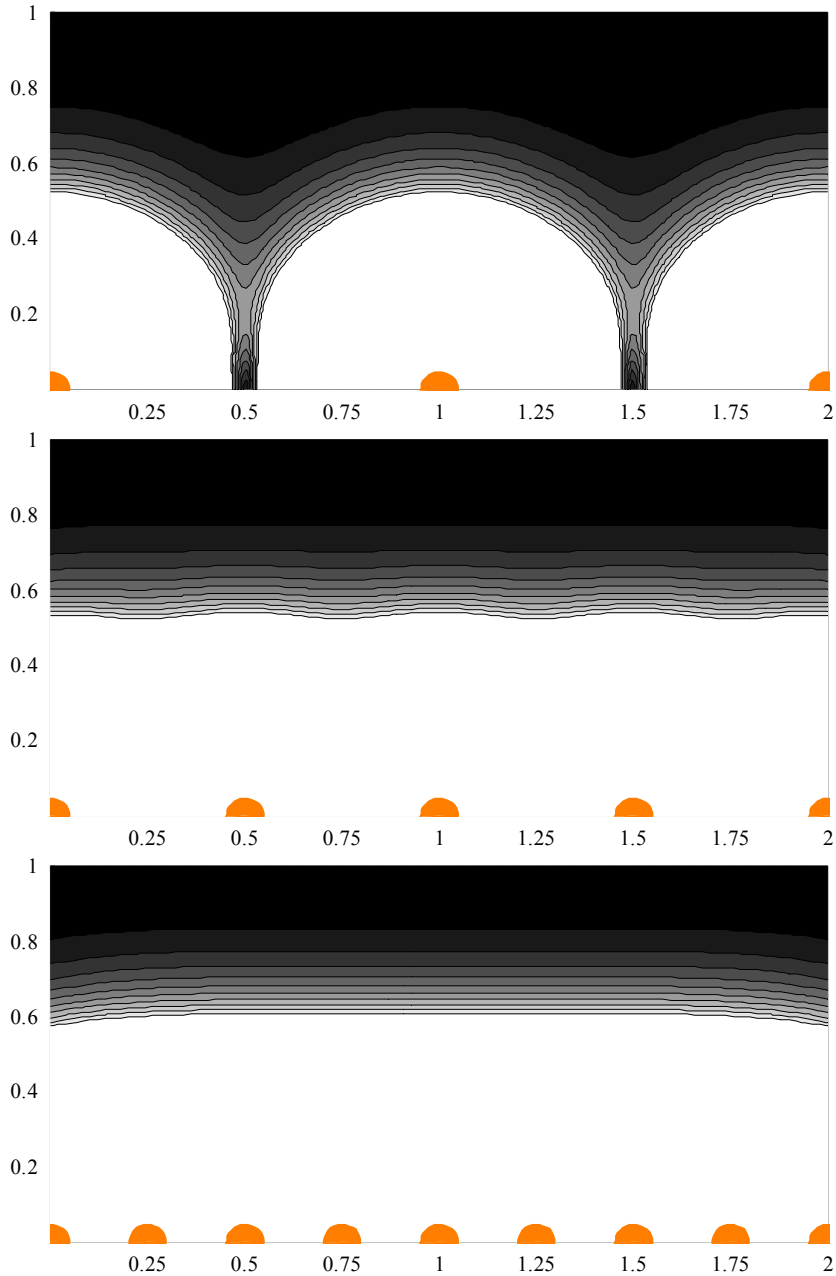

Fig. 1. boundary force field potential for ratios of boundary particle separation (radius of action of a) 1, b) ½ and c) ¼ .

One advantage of (6), is that the force on a boundary may be computed directly by integrating the forces – equal and opposite – produced by fluid particles on the boundary. This is the method to be used on the experiment in this paper.

3 PSEUDO – HIDROSTATIC TEST ON A RECTANGULAR CONTAINER

In order to check the accuracy and behaviour of the boundary method used, a preliminary test has been performed using a rectangular, 1.20 x 1.00 m container filled with 1.00 m of water, see fig. 2, measuring the time evolution of the horizontal force on one of its side-walls by adding the horizontal component of the fluid force on the wall particles. Fluid particles are laid on a rectangular lattice with spacing Δx = 0.02 m, for a total of 2,500 fluid particles. Boundaries are reproduced using particles with the same spacing and radius $r_0 = \Delta x$. The coefficients in (6) are given usual values with D = 50.

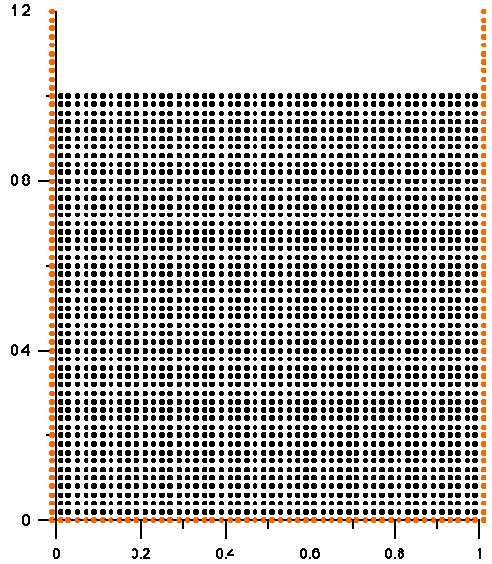

Fig. 2. Experimental setup for a pseudo hydrostatic test

Fluid particles are initialized with densities according to hydrostatic pressure in the experiment, that is according with:

$$\rho = \rho_0 \left(\frac{P\gamma}{c_s^2 \rho_0} + 1 \right)^{\frac{1}{\gamma}} \tag{7}$$

It is to be noted that no correction is made to the particle positions due to its changed density, and also that the particles do not experiment, in the initial instant, any force from the boundaries. Therefore, when the experiment starts, particles will fall due to gravity towards the boundaries, starting an elastic oscillation damped by viscosity. The experiment has been run for 20 seconds, using an explicit predictor – corrector method for integration of (3), a sound speed of 30 m/s and a time-step of around 2 10^{-4} s due to Courant number and other restrictions, see Monaghan (1992). A truncated on 3 h, normalized gaussian kernel, see Colagrossi and Landrini (2003) kernel has been used, with $h = \Delta x$. An standard viscosity coefficient and XSPH correction with ε = 0.5 have been used also.

Fig. 3 shows the raw force time series results on one wall obtained after each time step during the simulation, that confirms the regular dampened harmonic oscillator behaviour of the system. Force result converges towards an average value of 4,798 kN, with an small error of 2% respect the hydrostatic pressure to be expected on the wall.

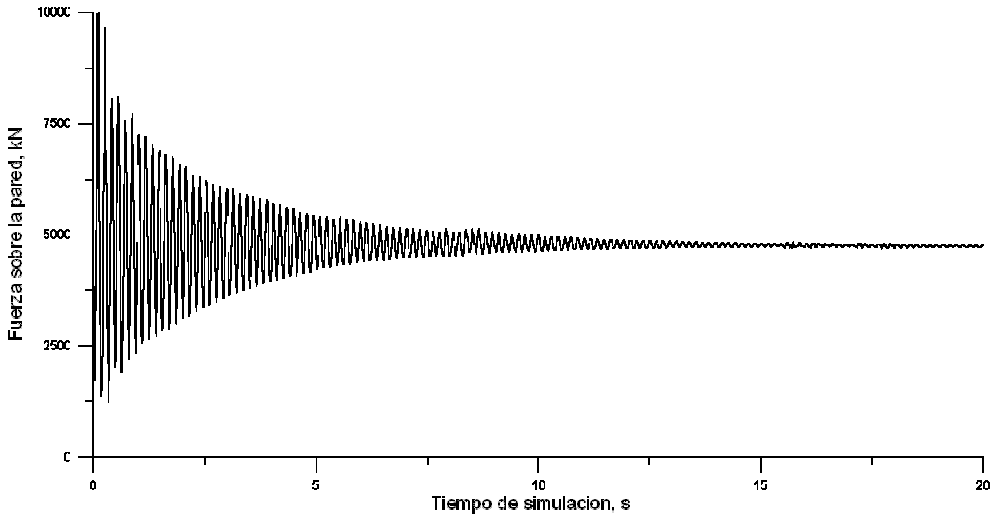

Fig. 3. Time series of total force on the container wall

Fig. 4 shows the amplitude of the frequency spectrum corresponding to the force signal, further confirming the behaviour shown by the time series. The characteristic frequency is of around 6 Hz and is to be related to the water depth (mass of the oscillator) and coefficient of the boundary force.

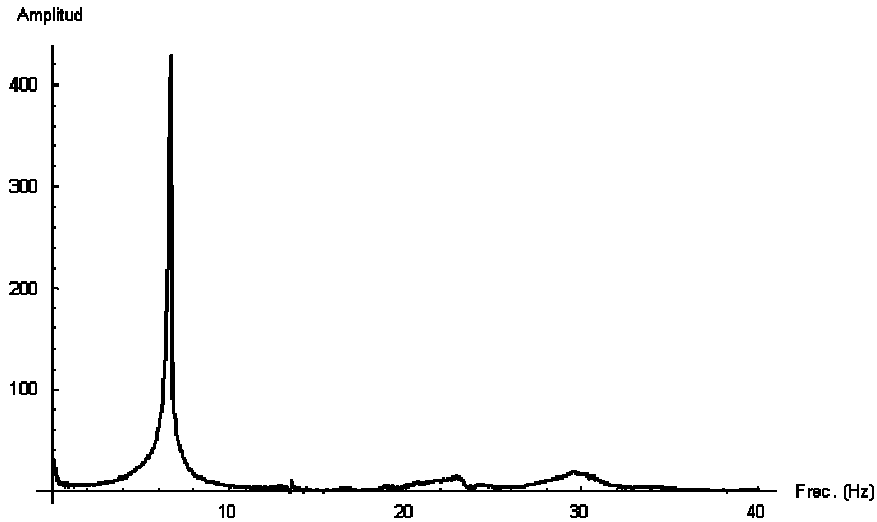

Fig. 4. Amplitude spectrum of force on the container wall

It is concluded that reliable estimates of integrated forces may be obtained through the direct procedure of adding boundary particle forces, and that the boundary condition generates an elastic motion behaviour on the fluid, with a characteristic frequency. While in a situation directed towards equilibrium such motion is progressively dampened, it is hypothesized that in a dynamic experiment the phenomenon may be permanently forced and then a certain amount of 'boundary noise' will be present.

4 SIMULATION OF FORCES ON A WAVE MAKER

The experiment has been simulated on a very short, 7 m long numerical wave flume with a one – meter wide horizontal bottom close to the wavemaker and a uniform 20% slope on the remaining length. Water depth in the wave flume is 1 m. In order to avoid as much as possible perturbations in the force measurements, wave conditions producing a plunging wave breaking and a reduced wave reflection of about 10% have been established, fixing wave conditions of 2 s period, 0.39 m of wave height and an Iribarren number of 0.79. Within such compromise it is to be noted that the wave is quite steep and therefore that limits in some sense the quality of linear theory wavemaker force prediction. The wave maker is of piston type, moving with the prescribed frequency and stroke of 0.34 m calculated for the desired

wave height according to linear wave theory. Figure 5 shows the experimental setup during the execution of an experiment.

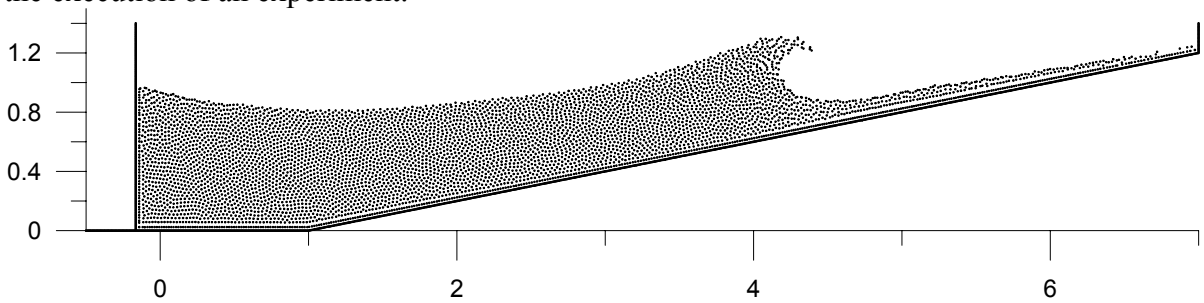

Fig. 5. Numerical wave flume during the experiment, t = 7.5 s

The simulations have been performed for a period of 20 s, taking for analysis the force data on the paddle in the interval from 6 to 20 s, last 7 waves, in order to avoid the initial disturbance due to the non-equilibrium between the fluid particles and boundary. Three experiments have been performed with refined resolution over the same setup and fluid particle spacing Δx = 10, 5, 2.5 cm. Boundary particle spacing has been, in each case, ¼ the spacing between fluid particles, with $r_0 = \Delta x$. It is to be noted that the first resolution implies only 10 fluid particles in the water column in front of the wave maker. The interest of assessing the performance of the technique with not too detailed resolution is remarkable for applications because of the associated computational cost; for this cases, on the same computer, the calculation time has went from less than one minute for the lowest resolution to slightly more than one hour for the highest.

The SPH implementation used, MDST, has been used with standard values according to section 3 in this paper, re-initializing also the density field values on the particles according to SPH smoothing (1) every 50 time steps. Time step ranges from 8 10^{-4} to 2 10^{-4} for the lower and upper resolutions. Figure 6 shows, for the last 14 s of the simulation with resolution Δx = 2.5 cm, the raw results time series and the theoretical $f(t)$ prediction (thick line, red in the electronic version) based on linear theory for a full draft paddle:

$$f(t) = \frac{\rho\, g\, d^2}{2} + \frac{\rho\, g\, a \sinh(k\, d)}{k} s \cos(\sigma\, t) + \rho\, \sigma \sum_{i=1}^{\infty} \frac{c_n}{k_n} s \sin(k_n d) \sin(\sigma\, t) \tag{8}$$

Where g is the gravity, d water depth, k and k_n real and modulus of complex roots of wave dispersion equation, σ the angular frecuency, s the total stroke of the wavemaker and the coefficients a, c_n have the following expressions:

$$\begin{aligned} a &= \frac{2\,\sigma}{k\,(\sinh(2\,k\,d)) + 2\,k\,d}\left(\sinh(k\,d) + \frac{1-\cosh(k\,d)}{k(d+l)}\right) \\ c_n &= -\frac{2\,\sigma}{k_n\,(\sinh(2\,k_n\,d)) + 2\,k_n\,d}\left(\sin(k_n\,d) + \frac{1-\cos(k_n\,d)}{k_n(d+l)}\right) \end{aligned} \tag{9}$$

Where the parameter l takes a value ∞ for a piston wave maker. According to (8) the force is composed of a permanent term, corresponding to hydrostatic force, plus a term associated to the progressive term and finally an infinite summation due to evanescent modes that arise due to the disagreement between paddle motions and water motion for a progressive wave. It is to be noted that the frequency for both the progressive and trapped terms is the same.

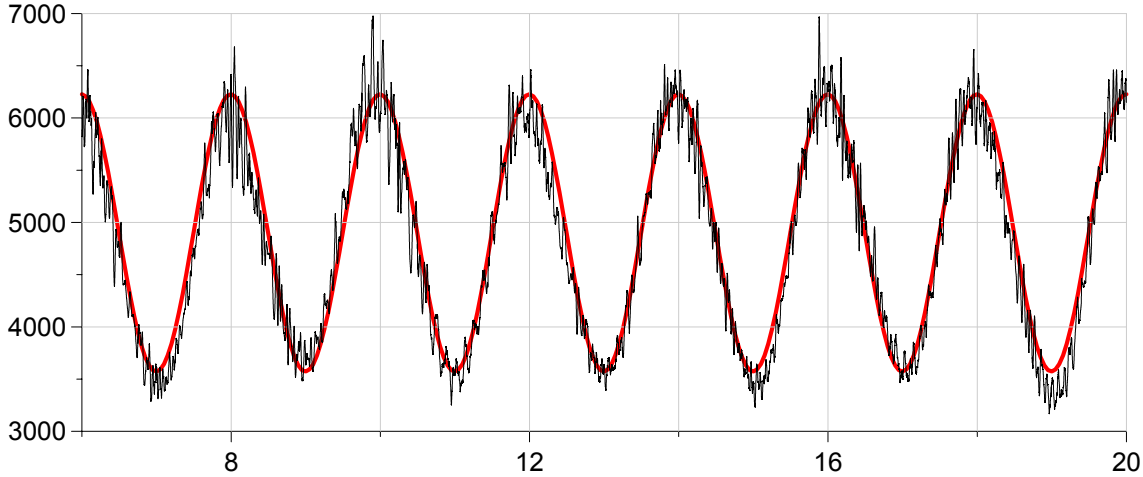

Fig. 6. Time series of forces (kN) on the wave maker during the time interval 6 – 20 s. Thicker line is the theoretical prediction

It is first observed the presence of rather stable along the experiment high frequency noise on the raw numerical experimental data. However, the overall result is in quite good agreement with the prediction, both in terms of amplitude and phase. It is also noted some long wave activity in the model that produces differences in elevation for successive crests and troughs of the force signal. In order to analyze quantitatively the signal, the complex amplitude spectrum of the force signal has been obtained in each case – a representation for the case with higher resolution is shown in figure 7. It may be seen the clear peak on the seventh band (corresponding to 0.5 Hz) of the spectrum as well as the well – defined second harmonic on the fourteenth band due to nonlinear effects. Some long wave activity is also to be noted, and noise develops in between 6 – 8 Hz and may be related probably to the boundary condition effects although its amplitude is not very significant when related to the main component of the force.

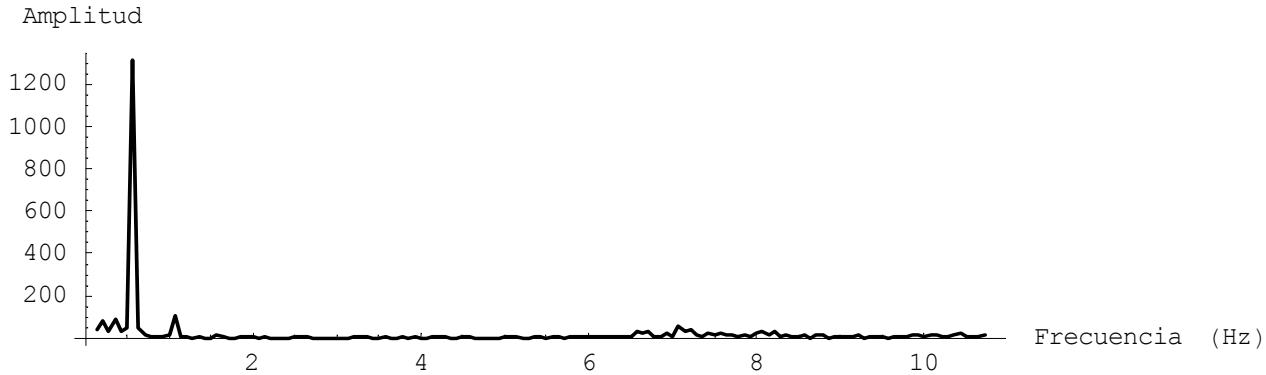

Fig. 6. Modulus of the complex amplitude spectrum for the raw force signal during the time interval 6 - 20 s.

Using the spectral estimates, table I has been composed, showing the theoretical results jointly with the experimental results for the average value of the force (4.900 kN hydrostatic component) and for the oscillatory force composed of the progressive plus the evanescent contributions whose predicted value is 1.327 kN. From the spectrum, the mean value is obtained as the zero frequency component, and the oscillatory amplitude value from the seventh band corresponding to 0.5 Hz.

Table I. Numerical simulation results and deviation from theoretical predictions

Δx, cm	*Mean value, kN*	*% deviation*	*Oscillatory amplitude, kN*	*% deviation*
10	4.446	-9.3	1.475	11.2
5	4.696	-4.2	1.331	0.58
2.5	4.818	-1.7	1.315	-0.90

From these results, it seems that the solution is already close to convergence, from an engineering point of view, for the intermediate resolution, with few changes on the highest resolution. This trend is more significant than the very small difference with linear theory – only an indication - in this case because of the uncertainties associated with reflection and non-linearity in the experiment, clearly larger than the difference between results.

In order to assess the effectiveness of the boundary spacing reduction applied, the experiment has been performed using a boundary spacing equal to the fluid particle spacing, and maintaining the same radius of action of the force. The results for the three resolutions of the oscillatory force component are, respectively, of 1.901, 1.612 and 1.474 kN, showing clearly the added –mass effect of the irregularity. It is to be noted that the best result, for the higher resolution, is of similar quality with the worst result (with the lowest resolution) when using a reduced spacing, thus confirming the usefulness of this approach.

5 CONCLUSION

Within the frame of verification of a numerical, SPH wave flume, the predictive capability of the method concerning the evaluation of forces produced by the fluid on a wave maker has been tested for a specific situation. The simple evaluation through the addition of forces on the boundary particles that form the wave maker have provided for this case a reasonable estimate, showing a good convergence even with a not too high resolution. The results may be considered satisfactory being noted that no effort has been devoted to adjust coefficients values in the model, using instead rather 'standard' values, thus testifying the model capabilities and robustness. Those results allows to expect similar levels of quality on more complex wave – structure interaction problems. However, this paper has analyzed only a single wave generation case and should be extended to a range of relative water depths, in particular covering cases with more significant contribution from evanescent modes and other types of wave generators like flap-type or combined piston – flap motion.

The results show clearly that the rough nature of the boundary force of Monaghan (1994) has an effect of added mass on the forces on the wave generator that may be corrected in a simple and efficient way by reducing the spacing between boundary particles but keeping at a larger value the radius of action of the boundary force. Even if this boundary technique requires an increased number of boundary particles, the dimensionality of the boundary is lower than that of the fluid domain in the experiment and therefore this may not be a severe computational constraint in most cases.

ACKNOWLEDGMENTS

Thanks are given to Prof. Moncho Gomez-Gesteira, Vigo Univ., for his friendly examination of a preliminary draft of this paper and for making very useful suggestions. This work has been partially funded by Puertos del Estado under project 24-405-9-163.

REFERENCES

Colagrossi and Landrini (2003), Numerical simulation of interfacial flows by smoothed particle hydrodynamics. Journal of computational physics, 191

Gomez-Gesteira, M. and Dalrymple, R.A. (2003), Analysis of single waves impact on coastal structures by means of a 3D SPH Method, in *Long Waves Symposium 2003, edited by Briggs, M. and Koutitas,Ch.* , pp. 1-10, IAHR – COPRI

Gómez-Gesteira, M. and Dalrymple, R.A. (2004), Using a 3D SPH Method for Wave Impact on a Tall Structure. J. Waterways, Port, Coastal and Ocean Eng., 130(2): 63-69.

Monaghan, J. (1992), Smoothed particle hydrodynamics. Annual review of astronomy and astrophysics, 30

Monaghan, J. (1994), Simulating free surface flows with SPH. Journal of computational physics, 110.

Monaghan, J., Kos, A. and Issa, N. (2003), Fluid motion generated by impact. Journal of Waterways, Port, Coastal and Ocean Engineering, Vol. 129, No. 6

Monaghan, J. (2005), Smoothed Particle Hydrodynamics. Reports on progress in physics, 68